

General Disclaimer

One or more of the Following Statements may affect this Document

- This document has been reproduced from the best copy furnished by the organizational source. It is being released in the interest of making available as much information as possible.
- This document may contain data, which exceeds the sheet parameters. It was furnished in this condition by the organizational source and is the best copy available.
- This document may contain tone-on-tone or color graphs, charts and/or pictures, which have been reproduced in black and white.
- This document is paginated as submitted by the original source.
- Portions of this document are not fully legible due to the historical nature of some of the material. However, it is the best reproduction available from the original submission.

(NASA-TM-80278) A MODEL FOR THE MICROWAVE
EMISSIVITY OF THE OCEAN'S SURFACE AS A
FUNCTION OF WIND SPEED (NASA) 25 p
HC A02/MF A01

N79-27640

CSCCL 08C

G3/43
Unclas
29961



Technical Memorandum 80278

A Model for the Microwave Emissivity of the Ocean's Surface as a Function of Wind Speed

Thomas T. Wilheit

April 1979

National Aeronautics and
Space Administration

Goddard Space Flight Center
Greenbelt, Maryland 20771



**A MODEL FOR THE MICROWAVE EMISSIVITY OF
THE OCEAN'S SURFACE AS A FUNCTION OF WIND SPEED**

**Thomas T. Wilheit
Goddard Space Flight Center
Greenbelt, Maryland**

ABSTRACT

A quantitative model is presented which describes the ocean surface as an ensemble of flat facets with a normal distribution of slopes. The variance of the slope distribution is linearly related to frequency up to 35GHz and constant at higher frequencies. These facets are partially covered with an absorbing nonpolarized foam layer. Experimental evidence is presented for this model.

CONTENTS

	<u>Page</u>
ABSTRACT	iii
INTRODUCTION	1
THE MODEL	5
SUPPORTING OBSERVATIONS	8
LIMITATIONS OF THE MODEL	9
CONCLUSION	15
REFERENCES	17

ILLUSTRATIONS

<u>Figure</u>	<u>Page</u>
1 The Effect of an Absorbing Layer on a Microwave Radiance Expressed as a Brightness Temperature Where T_B Is the Brightness Temperature, γ , δ , and t_0 the Absorption Coefficient, Thickness and Thermodynamic Temperature of the Layer	1
2 The Effect of Reflection of a Microwave Radiance Expressed as a Brightness Temperature Off a Surface Such as the Ocean Where T_\downarrow Is the Downwelling Brightness Temperature, T_\uparrow the Upwelling Brightness Temperature and E , R and t_{surf} the Emissivity, Reflectivity and Thermodynamic Temperature of the Surface Respectively.	2
3 Schematic Superposition of the Spectra of Various Geophysical Parameters, P_i . The arrows indicate the SMMR frequencies. The signs have been chosen to be positive in the frequency range of primary importance to the given parameter.	4
4 Emissivity as a Function of View Angle for a Smooth Water Surface and for the Ocean Surface with 7 and 14m/s Wind Speed	6
5 Observed Value of $F_{285} = (T_H - 285)/(T_V - 285)$ and Wind Speeds. The geometric optics curve is based on the Cox and Munk ¹² distribution of surface slopes.	10

PRECEDING PAGE BLANK NOT FILMED

ILLUSTRATIONS (Continued)

<u>Figure</u>	<u>Page</u>
6 Percentage of Cox and Munk ¹² Slope Variance Required for a Geometric Optics Model to Explain the Nimbus-6 Observations ¹⁴ (X) and Hollinger ¹⁵ (●) as a Function of Frequency	11
7 Frequency Dependence of the Extent to Which Wind Induced Foam Reduces the Microwave Emissivity of the Ocean Surface	12
8 Brightness Temperature Increase Due to Wind Speed at 2.65 GHz from Blume, et al. ¹⁸	13
9 Foam Coverage Efficiency Calculated with a 6 mm Linear Index of Refraction Transition and a 1 cm Weakly Absorbing Layer	14
10 Approximate Error in Vertical Emissivity at 100% Foam Cover Due to Ignoring Polarization Properties of Foam	16

A MODEL FOR THE MICROWAVE EMISSIVITY OF THE OCEAN'S SURFACE AS A FUNCTION OF WIND SPEED

INTRODUCTION

The Scanning Multichannel Microwave Radiometer (SMMR) is a five frequency (6.6, 10.7, 18, 21, and 37GHz) dual polarized microwave radiometer which was carried aboard the Nimbus-7 and Seasat satellites both of which were launched in 1978. The instrument has an 80 cm parabolic dish antenna which scans its main beam 50° in azimuth along a conical surface with a 42° cone angle and a vertical axis. This provides a constant incidence angle of approximately 50° at the Earth's surface for the orbital altitudes of the two spacecraft (ca 600km Seasat, 800km Nimbus). The spatial resolution is proportional to wavelength and varies from approximately 150km at 6.6GHz to 25km at 37GHz. The instrument has been described in detail by Gloersen and Barath.¹ The purpose of this instrument is to measure sea surface temperature and wind speed at the sea surface globally even in the presence of clouds and light rain.

The SMMR, being a radiometer, measures the upwelling thermal microwave radiation, the intensity of which is characterized by a brightness temperature. The physical significance of a brightness temperature is illustrated in Figure 1. If microwave radiation with an intensity characterized

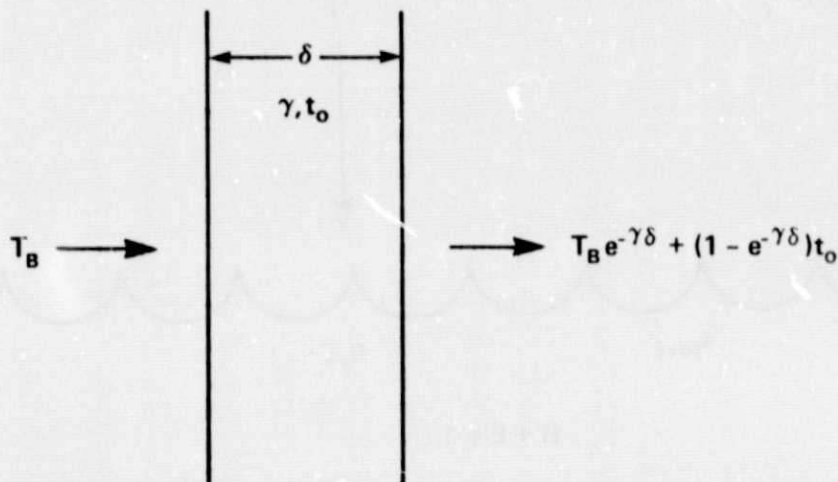


Figure 1. The Effect of an Absorbing Layer on a Microwave Radiance Expressed as a Brightness Temperature Where T_B Is the Brightness Temperature, γ , δ , and t_0 the Absorption Coefficient, Thickness and Thermodynamic Temperature of the Layer

by T_B is incident on an absorbing (but not scattering or reflecting) layer with an absolute thermodynamic temperature t_0 , an absorption coefficient γ and a thickness δ , the intensity coming out the other side is given by:

$$T'_B = T_B e^{-\gamma\delta} + t_0(1 - e^{-\gamma\delta}) \quad (1)$$

That is, T'_B is given by a term representing the attenuation of the incident radiation and a complementary radiation term proportional to the absolute temperature of the absorber (Rayleigh-Jeans approximation). Note that if $T_B = t_0$ the intensity of the radiation is unchanged; the radiation is in equilibrium with the absorber. The layer in question could be a section of waveguide, an antenna, a radome, or a substantially uniform portion of the atmosphere. For computation purposes, the atmosphere is typically treated as many such layers.

A similar relationship holds for reflection at a surface as is illustrated in Figure 2. If the downwelling radiation is given by T_\downarrow then the radiation upwelling off the surface T_\uparrow is given by

$$T_\uparrow = RT_\downarrow + Et_s \quad (2)$$

where R is the power reflectivity of the surface, E is the emissivity of the surface and t_s is the

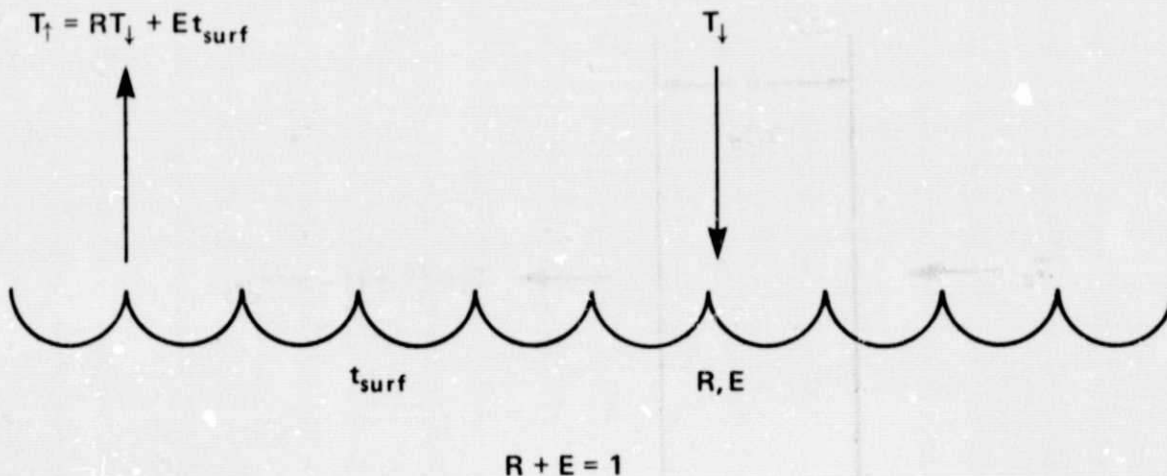


Figure 2. The Effect of Reflection of a Microwave Radiance Expressed as a Brightness Temperature Off a Surface Such as the Ocean Where T_\downarrow Is the Downwelling Brightness Temperature, T_\uparrow the Upwelling Brightness Temperature and E , R and t_{surf} the Emissivity, Reflectivity and Thermodynamic Temperature of the Surface Respectively

absolute thermodynamic temperature of the surface. Consideration of thermodynamic equilibrium requires that

$$R + E = 1 \quad (3)$$

The absorption properties of the atmosphere have been discussed by Chang and Wilheit.² The dominant features in the frequency range of interest here are a weak water vapor resonance centered at 22.235GHz and absorption due to non-raining clouds which is approximately proportional to the square of the frequency. The entire problem of radiative transfer in the presence of rain is much more complicated as scattering as well as absorption must be considered.³ The reflection and emission properties of the ocean surface are the subject of this paper. Figure 3 is a schematic superposition of the spectra of all the parameters of interest here. The ordinate is the partial derivative of the upwelling brightness, temperature with respect to the parameter of interest, $\frac{\partial T_B}{\partial P_i}$, expressed in arbitrary units. The polarity has been chosen to make the effect positive where it is important. The frequencies of the SMMR are marked with the arrows. One can see that these are well chosen frequencies for sorting out these effects. There is also some information content in the polarization of the brightness temperatures but that is not so easily displayed; it is however implicitly exploited in schemes to retrieve the various parameters from the brightness temperature measurements.^{2,4,5,6} Simulations based on these retrieval schemes and measured performance of the SMMR instrument^{4,5,6} indicate that a measurement accuracy of 1.5°C is attainable for the sea surface temperature. The lowest frequency, 6.6GHz, is used in this retrieval thus the spatial resolution is limited to roughly 150km. Similarly, the surface wind speed can be extracted from the measurements to roughly 1 m/s accuracy. The lowest frequency used for surface wind speed is 10.7GHz, so approximately 90km spatial resolution is attained. Atmospheric water can be retrieved with a spatial resolution of 60km and an accuracy of 0.15gm/cm² and 4mg/cm² for the vapor and liquid phases respectively.

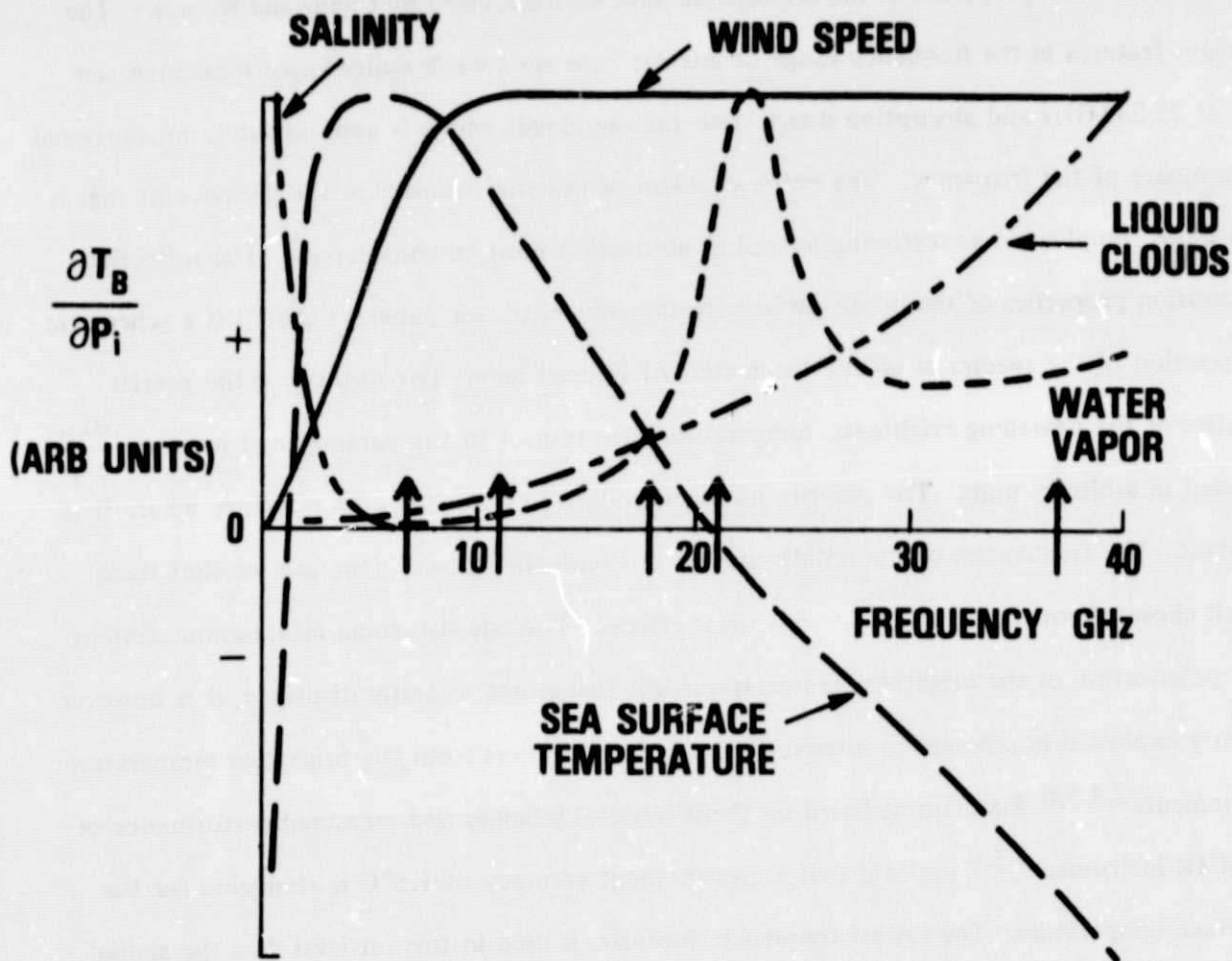


Figure 3. Schematic Superposition of the Spectra of Various Geophysical Parameters, P_i . The arrows indicate the SMMR frequencies. The signs have been chosen to be positive in the frequency range of primary importance to the given parameter.

In the various discussions^{2,4,5,6} of the retrieval schemes, it is obvious that the only significant uncertainty in the required modelling is the effect of the wind on the microwave emissivity of the oceans surface. The purpose of this paper is to document the model used in the version of the retrieval algorithm⁶ used at launch of the two spacecraft, to justify this model as well as possible and to examine its limitations.

THE MODEL

It is a straightforward problem to calculate the emissivity of a smooth water surface. The dielectric properties of sea water and saline solutions have been discussed by many authors.^{7,8,9} We will use values derived from the Lane and Saxton⁷ measurements and expressed in an analytic form by Chang and Wilheit.² The formalism for calculating the emissivity for a given view angle and polarization is the so called Fresnel relations.¹⁰ The resulting emissivity as a function of view angle is shown in Figure 4 for a frequency of 10.7GHz and a temperature of 285°K. This smooth surface model was also used for calculating the surface temperature and salinity sensitivity curves shown in Figure 3. They were calculated for a view angle of 50° and vertical polarization; the results are similar for other angles and for horizontal polarization.

However, the ocean's surface is not a smooth surface; the wind roughens the surface, and, if it is blowing hard enough, partially covers the surface with foam. It is necessary at this point to define more precisely what is meant by surface wind speed. The wind varies with height near the surface and the details of this variation depend on the temperature difference between the air and the sea.¹¹ When the air is warmer than the ocean (stable) there is more wind shear than for the opposite (unstable) case for a given wind speed at some reference level. The wind for our purpose is measured near the surface ($\leq 200\text{m}$) along with the air and sea temperatures. These data are then used to calculate the so-called friction velocity U^* at the sea surface by means of the Cardone¹¹ model. This is then transformed to 20m height assuming that the sea and air temperature are equal (neutral stability). This last step is simply a one-for-one transformation to

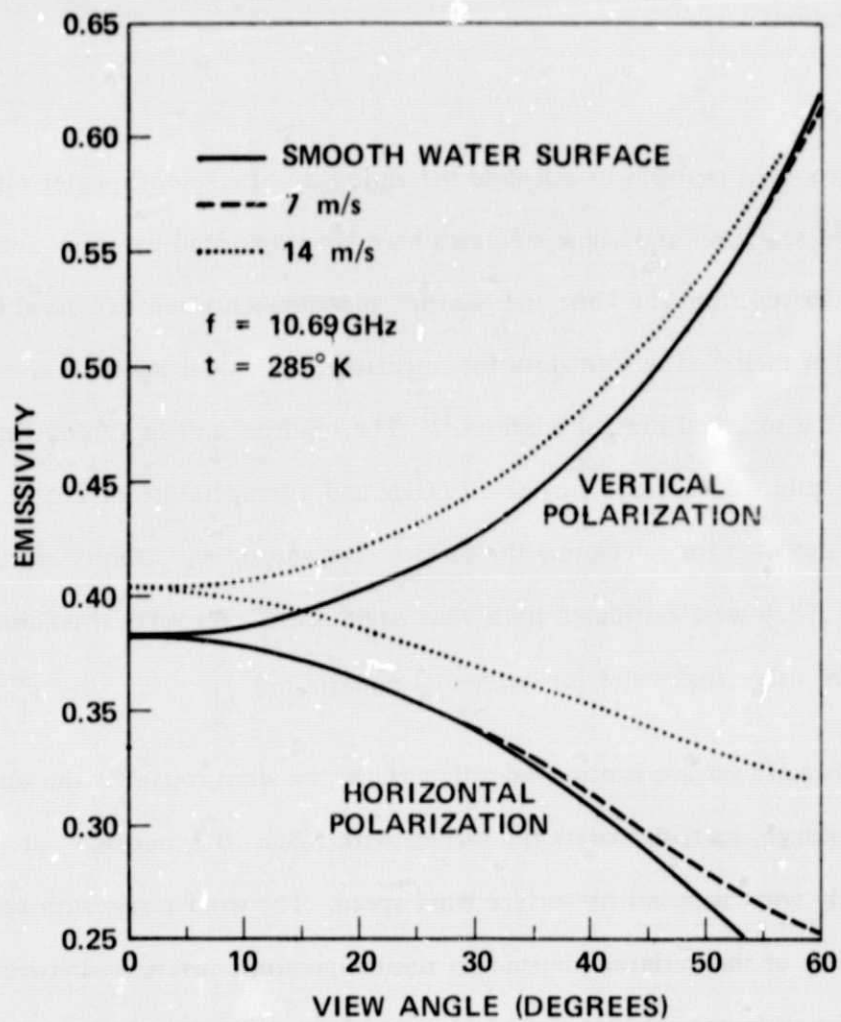


Figure 4. Emissivity as a Function of View Angle for a Smooth Water Surface and for the Ocean Surface with 7 and 14 m/s Wind Speed

express the friction velocity in more familiar terms. Wherever possible in this paper the winds have been converted to this 20 meter neutral stability wind.

Cox and Munk¹² have quantitatively described the distribution of surface slopes as a function of wind speed. They found that the surface slopes were normally distributed with a variance, given by

$$\sigma_{\zeta_m}^2 = 0.003 + 0.048W \quad (4)$$

where W is the wind speed in meters/seconds at 20m height. The factor multiplying W in the above equation is slightly different from that in the Cox and Munk¹² paper because the winds were measured at 12.5M in their work. These measurements were made at visible wavelengths. Much of the roughness they observed is at scales very small compared to microwave wavelengths. The model presented here requires only a fraction of the Cox and Munk roughness at the longer microwave wavelengths. Specifically, the slope variance observed at a given microwave frequency is:

$$\begin{aligned} \sigma^2(f) &= (0.3 + 0.02f(\text{GHz}))\sigma_{\zeta_m}^2 & f < 35\text{GHz} \\ \sigma^2(f) &= \sigma_{\zeta_m}^2 & f \geq 359\text{Hz} \end{aligned} \quad (5)$$

To calculate a rough surface emissivity from this slope distribution, one simply averages the Fresnel relations¹⁰ over the distribution of surface slopes. In doing so, one implicitly ignores surface curvature and all structure comparable to a wavelength and thereby reduces the problem to geometric optics. The comparison with observations which follow will demonstrate that this is a surprisingly good approximation.

Wind also creates foam on the ocean's surface. Nordberg, et al.,¹³ found a linear increase in brightness temperature with wind speed whenever the wind speed exceeded 7m/s. They were viewing directly at the nadir which essentially eliminates the roughness effect leaving foam as the most reasonable explanation. In our model, we will treat foam as partially obscuring the surface

in a manner independent of polarization. A non-reflecting material partially covering the surface would have this property as would an absorbing but partially transparent medium with the same temperature as the water. Either description alone would be inadequate, but a combination of the two descriptions would be closer to reality. The degree to which foam obscures the surface is frequency dependent and proportional to the amount by which the wind speed exceeds 7 m/s. A reasonable approximation to the available observations of the fraction, K , by which the surface reflectivity is reduced by foam is:

$$\begin{aligned} K &\cong a(1 - e^{-f/f_0})(w - 7 \text{ m/s}) & w \geq 7 \text{ m/s} \\ K &= 0 & w < 7 \text{ m/s} \end{aligned} \quad (6)$$

where f is the frequency

and $a = 0.006 \text{ s/m}$

$$f_0 = 7.5 \text{ GHz}$$

Emissivities calculated according to this model for 7 and 14 m/s are shown in Figure 4 for comparison with the emissivity of a smooth surface.

SUPPORTING OBSERVATIONS

Because the assumed foam model has no polarization character, dual polarized observations of the surface provide a test of the rough surface portion of the model. If one makes the approximation that the atmosphere and the surface have the same thermodynamic temperature T_1 , then it is straightforward to show that for any given view angle

$$F_{T_1}(\theta) = \frac{T_H(\theta) - T_1}{T_V(\theta) - T_1} = \frac{R_H(\theta)}{R_V(\theta)} \quad (7)$$

Here $T_H(\theta)$ is the horizontal brightness temperature at an angle and $R_H(\theta)$ is the horizontally polarized reflectivity. $T_V(\theta)$ and $R_V(\theta)$ refer similarly to vertical polarization. Note that because $F_{T_1}(\theta)$ is the ratio of two reflectivities, it is independent of foam cover and thus provides a measurement of surface roughening. The data from the Electrically Scanned Microwave Radiometer

(ESMR) on Nimbus-6 (37GHz, 50° view angle) have been so analyzed and compared with wind speeds derived from the operational data buoys.¹⁴ A summary of this comparison is given in Figure 5. The plotted data are for the most part, averages of many observations; a total of 264 observations are represented. In analyzing the data, it was found that a value of 285°K for T_1 worked best but that the improvement over any value in the range 280°K was only marginal. Using the model described in the previous section the expected value of F_{285} has been calculated: the agreement with the observations is striking. A geometric optics model using the Cox and Munk sea surface slope distribution works extremely well at a wavelength of 0.8cm and a view angle of 50°. Hollinger¹⁵ has made observations from a fixed platform at frequencies of 1.4, 8.36, and 19.34GHz. He has filtered the data to remove most of the foam effect but application of an analysis technique similar to that applied to the Nimbus-6 ESMR data certainly removes the remainder. These data all can be interpreted in terms of the geometric optics model but with much less slope variance than the Cox and Munk¹² values.

The fractions of the Cox and Munk slope variance required to account for the Hollinger¹⁵ data at 55° incidence angle are plotted in Figure 6. The Hollinger data are consistent with these roughness fractions for all view angles between 0 and 55°. The Nimbus-6 ESMR¹⁴ result is also shown in Figure 6. These data form a picture consistent with the roughness required in Equations (5) (shown as a solid line).

The primary available observations relevant to the effect of foam on surface emissivity are from the Bering Sea Expedition (BESEX)¹⁶ and from Cosmos 243.¹⁷ These results, along with a plot of $\partial K/\partial W$ is given in Figure 7. The observations are difficult but nevertheless show reasonable self-consistency except possibly for the one BESEX point at 37GHz.

LIMITATIONS OF THE MODEL

There are two obvious limitations to this model, the lack of physical optics effects and the simplistic treatment of foam. If one calculates the nadir emissivity of the surface according to the

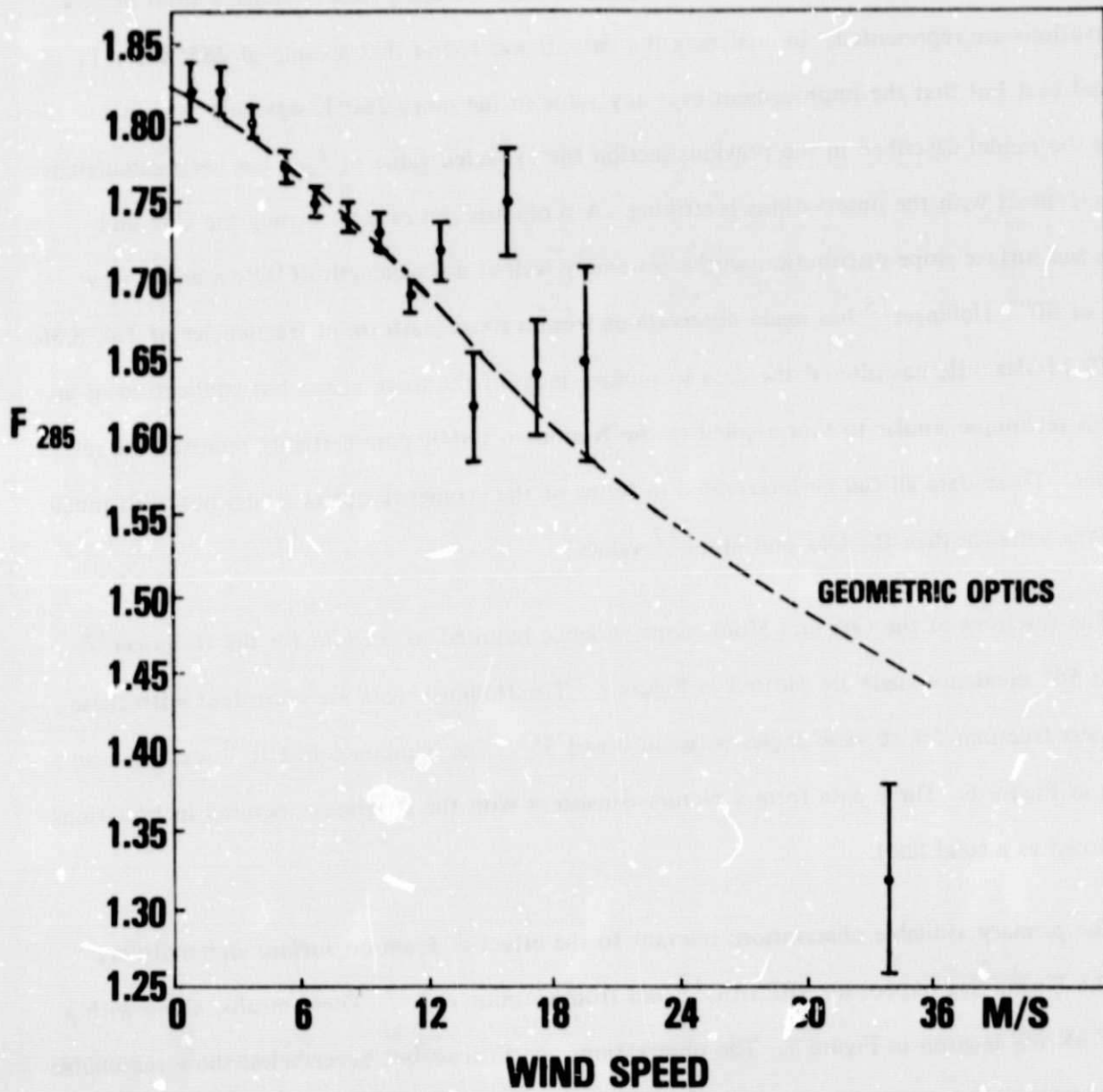


Figure 5. Observed Value of $F_{285} = (T_H - 285)/(T_V - 285)$ and Wind Speeds. The geometric optics curve is based on the Cox and Munk¹² distribution of surface slopes.

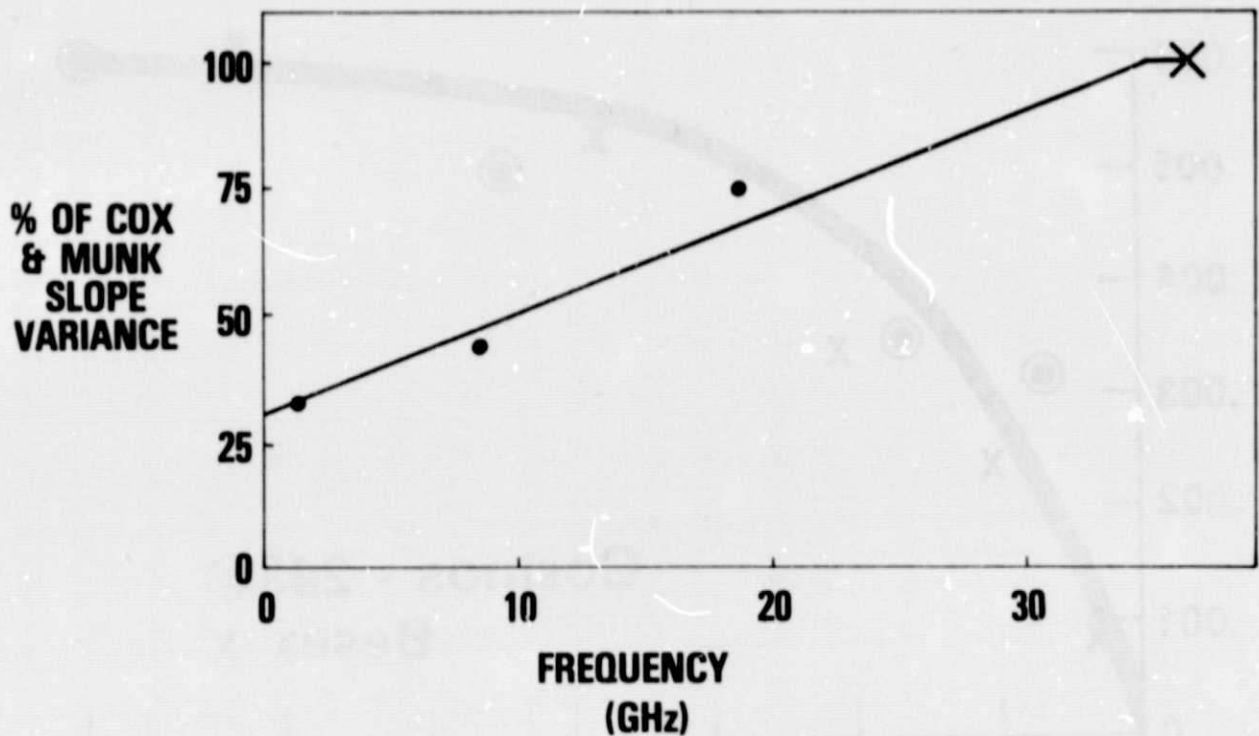


Figure 6. Percentage of Cox and Munk¹² Slope Variance Required for a Geometric Optics Model to Explain the Nimbus-6 Observations¹⁴ (X) and Hollinger¹⁵ (●) as a Function of Frequency

present, geometric optics, model there is substantially no change in emissivity through the entire 0-7 m/s wind speed range. Blume, *et al.*,¹⁸ have published the observations in Figure 8. These observations at 2.65GHz show a brightness temperature increase with increasing wind speed of approximately 0.2° K/m/s which corresponds to an apparent emissivity increase of 7×10^{-3} s/m. Even if one allows for the finite antenna beamwidth (20.5°) and the increasing contribution of reflected sky emission with increasing wind induced roughness, only about a quarter of this effect can be accounted for. There was not sufficient data in the paper¹⁸ to permit detailed calculations of the reflected solar radiation. The numbers are of the right order of magnitude to account for much of the observed effect. In any case, these observations suggest an upper limit to the physical optics contribution of about 5×10^{-3} s/m.

The treatment of foam here as having neither polarization properties nor any view angle dependence is clearly too simple. Williams¹⁹ has investigated the properties of gelatin stabilized

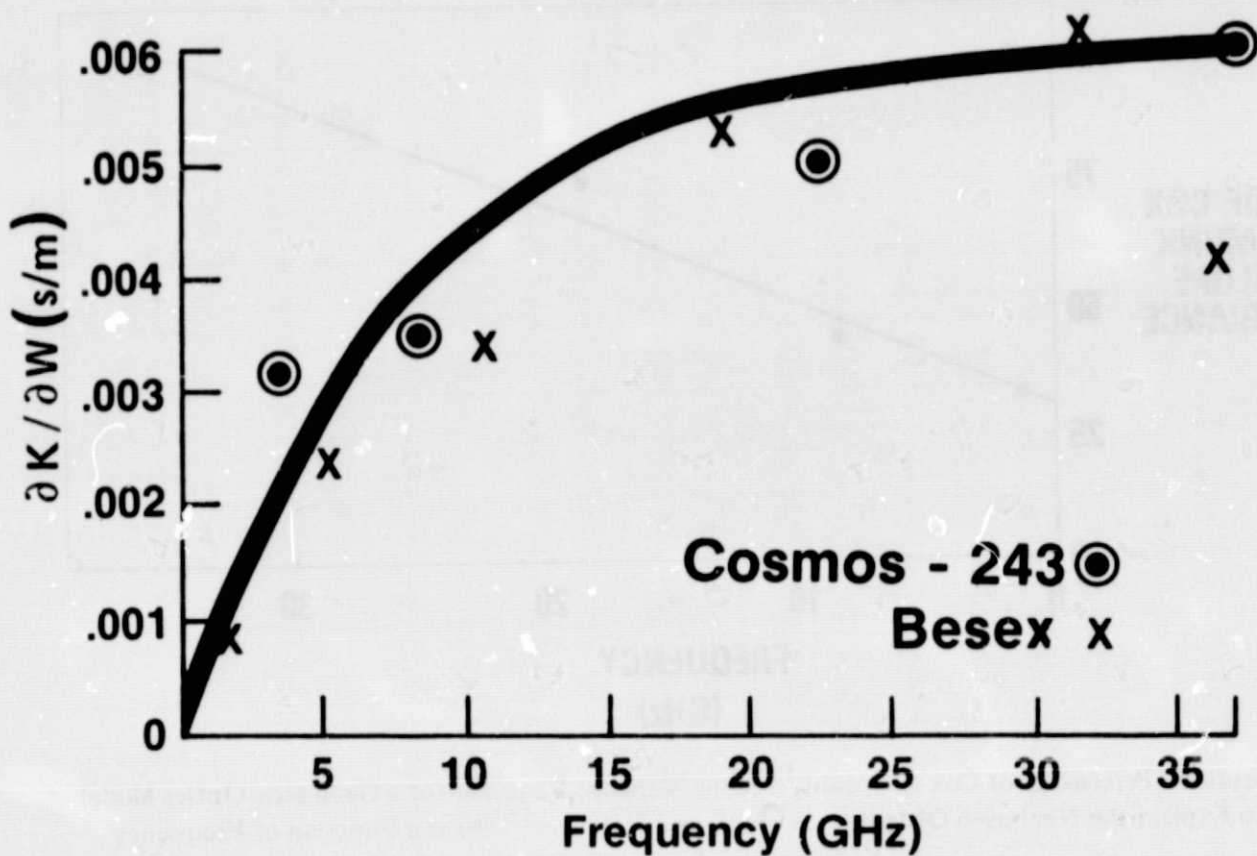


Figure 7. Frequency Dependence of the Extent to Which Wind Induced Foam Reduces the Microwave Emissivity of the Ocean Surface

bubble rafts under laboratory conditions. His results suggest that the increase of emissivity caused by foam is caused by the distortion of the meniscus at the foam-water interface which provides a gradual transition from the dielectric constant of air to that of water. His results with bubble rafts on an aluminum surface suggest that in the bulk of the foam the imaginary part of the index of refraction is on the order of 1% that of water. His results form the basis of a calculation of foam emissivity to be used as a credibility check on our foam description. Specifically we assume a 1 cm thick layer with a complex index of refraction.

$$n_{\text{foam}} = (n_{\text{water}} - 1)/100. \quad (8)$$

where n_{water} is the complex index of refraction of water, to represent the bulk of the foam and a linear transition from n_{foam} to n_{water} to represent the meniscus. The thickness of this linear

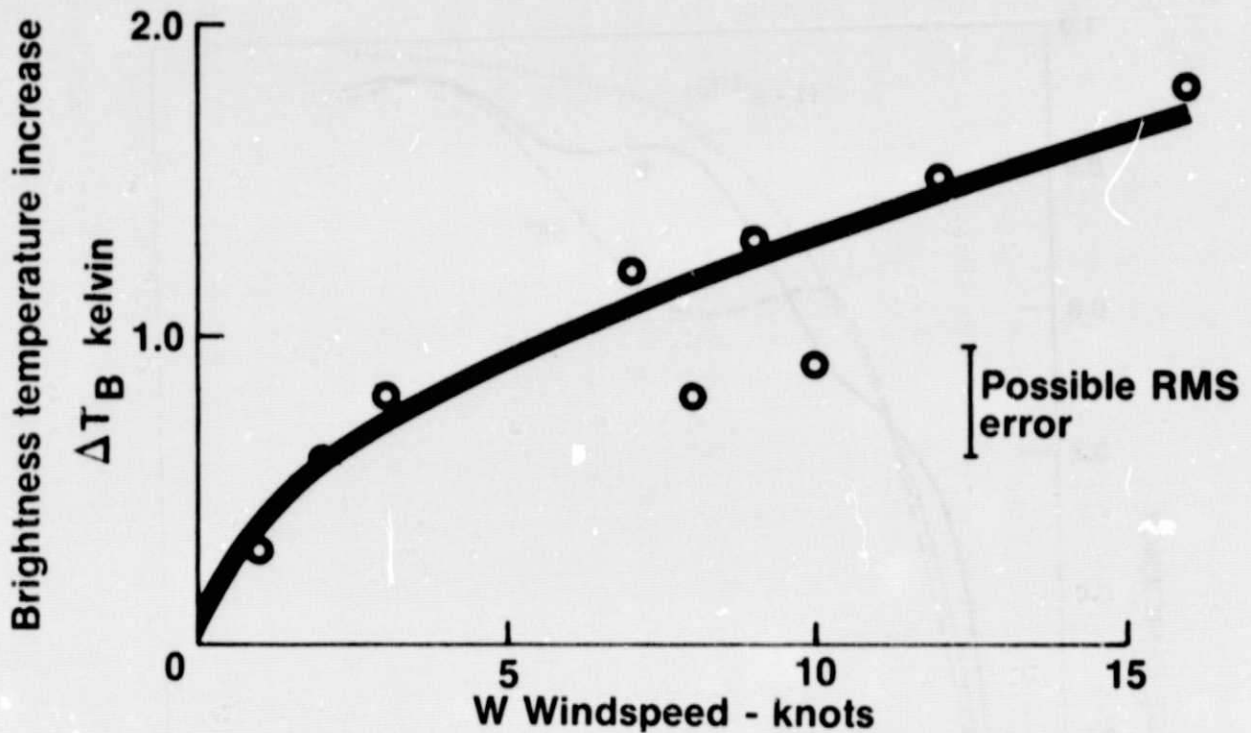


Figure 8. Brightness Temperature Increase Due to Wind Speed at 2.65GHz from Blume, et al.¹⁸

transition (0.6cm) was adjusted to provide a reasonable fit to the value of f_0 used in Equation (6). The emissivity of this was calculated²⁰ as a function of frequency and view angle. The foam coverage efficiency, E_F , was defined in terms of the horizontally polarized emissivity of the foam E_H^{foam} and of smooth water E_H^{water}

$$E_F \equiv \frac{E_H^{\text{foam}} - E_H^{\text{water}}}{1 - E_H^{\text{water}}} \quad (9)$$

Foam coverage efficiencies so calculated are shown in Figure 9 for view angles of 5° and 55° . The foam coverage efficiency implied in Equation (6), $(1 - e^{-f/f_0})$, is shown for comparison. Except for some structure which is an artifact of the calculation, (resonances within the 1 cm foam layer) and which certainly would not be observed in natural foam, the agreement is reasonable suggesting that ignoring view angle effects in our description of foam may not be too serious.

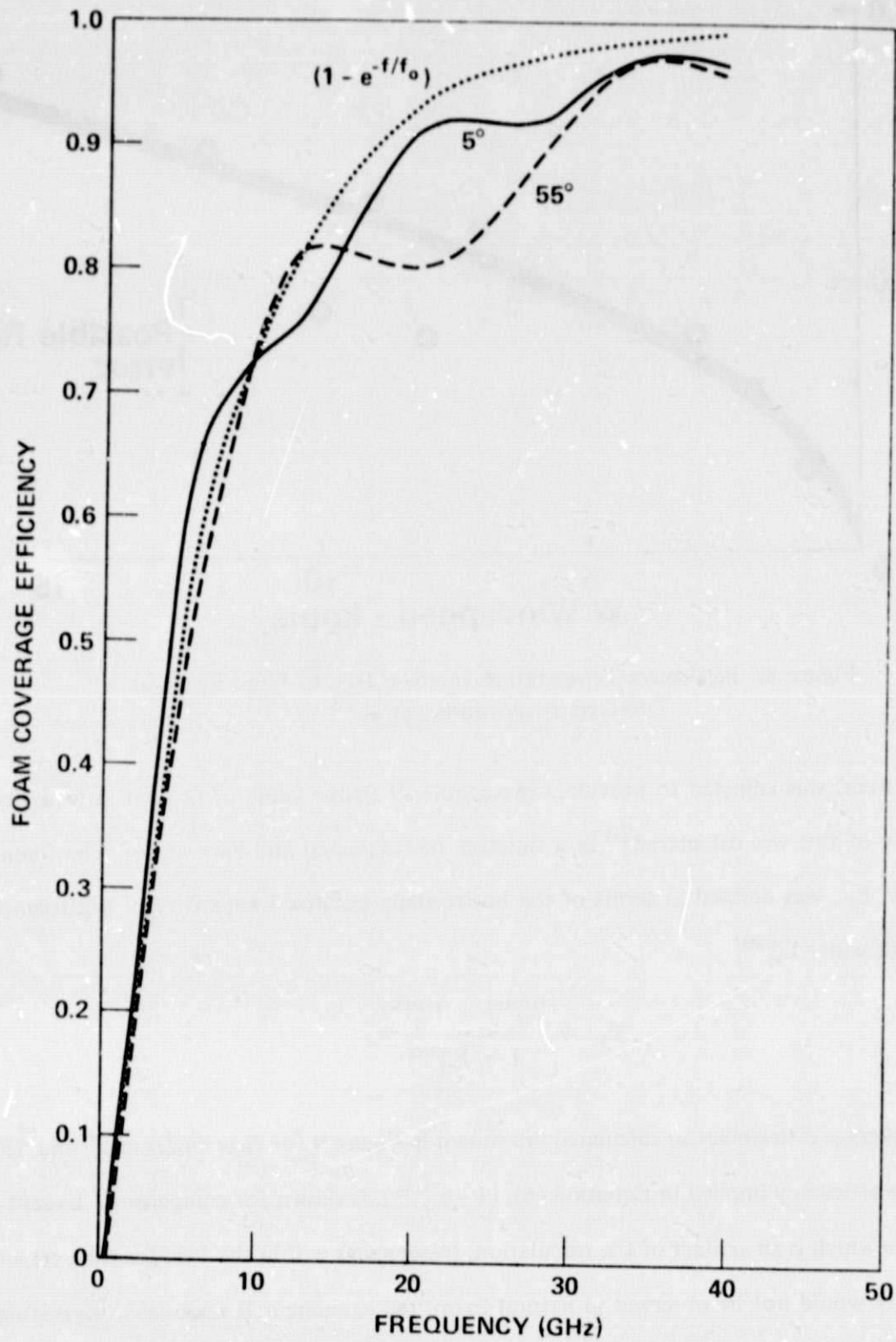


Figure 9. Foam Coverage Efficiency Calculated with a 6mm Linear Index of Refraction Transition and a 1cm Weakly Absorbing Layer

The lack of polarization character in the foam is more serious. By assuming that foam merely partially obscures the surface we are assuming that the horizontal and vertical reflectivities are reduced in the same proportion, i.e.:

$$1 - E_V^{\text{foam}} = \frac{(1 - E_H^{\text{foam}})(1 - E_V^{\text{water}})}{(1 - E_H^{\text{water}})} \quad (10)$$

In Figure 10, the vertical emissivity error made in this assumption is shown for view angles of 45° and 55° . The error is less for smaller angles and vanishes identically for 0° . The resonances observed in Figure 9 are observed in Figure 10 and must be similarly discounted. Nevertheless errors of about 0.05 in the vertical emissivity would be expected for 100% foam cover (wind speed greater than 170m/s). The sign of the error is such that the true emissivity in vertical polarization is somewhat greater than Equation (10) would suggest.

CONCLUSION

A model has been presented for the microwave emissivity of a wind roughened, foam covered ocean. The roughness portion of the description is remarkably consistent with observations; the foam effects show somewhat more scatter. The strength of the foam cover effect at 6.6 and 10.7 GHz are important parameters in the interpretation of Nimbus-7 and Seasat SMMR data; the strength at higher frequencies less so. In comparing the space observations with surface measurements of temperature and wind speed, it should be possible to adjust the foam effect at these two frequencies in order to fine-tune the retrieval algorithm.

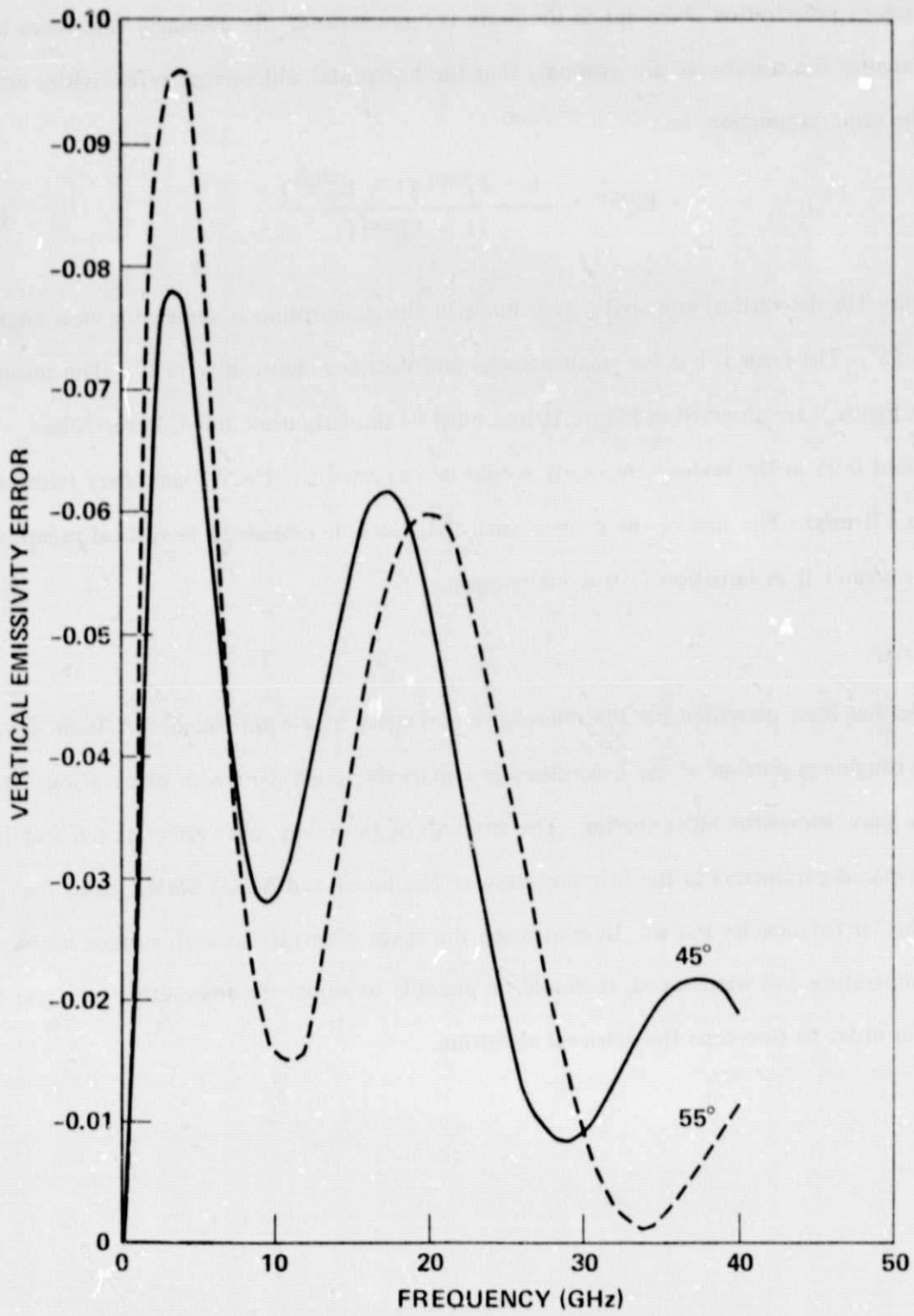


Figure 10. Approximate Error in Vertical Emissivity at 100% Foam Cover Due to Ignoring Polarization Properties of Foam

REFERENCES

1. Gloerson, P. and F. T. Barath, 1977: A scanning multichannel microwave radiometer for Nimbus-G and Seasat-A. Trans IEEE (OE). OE-2, 172-178.
2. Chang, A. T. C. and T. T. Wilheit, "Remote Sensing of Atmospheric Water Vapor, Liquid Water, and Wind Speed at the Ocean Surface by Passive Microwave Techniques From the Nimbus-5 Satellite," NASA TM-79568, June 1978, to be published in Radio Science.
3. Wilheit, T. T., A. T. C. Chang, M. S. V. Rao, E. B. Rodgers, and J. S. Theon: "A Satellite Technique for Quantitatively Mapping Rainfall Rates Over the Oceans," J. Appl. Meteor., 16, 551-650, (1977).
4. Wilheit, T. T.: "A Review of Applications of Microwave Radiometry to Oceanography," Bdy. Layer Met., 13, 277-293, (1978).
5. Wilheit, T. T.: "Atmospheric Corrections to Passive Microwave Observations of the Ocean," Invited Paper Presented at the Inter Union Commission on Radio Meteorology Colloquium on Passive Radiometry of the Ocean's Surface," Patricia Bay, B. C., Canada, 1978, to be published in Bdy. Layer Met.
6. Wilheit, T. T. and A. T. C. Chang: "An Algorithm for the Retrieval of Surface and Atmospheric Parameters from the Observations of the Scanning Multichannel Microwave Radiometer (SMMR) Over Oceans," NASA TM-80277, (1979).
7. Lane, J. A. and J. A. Saxton, "Dielectric Dispersion in Pure Polar Liquids at Very High Radio Frequencies," Proc. Roy. Soc., London A, 214, pp. 531-545, (1952).
8. Kline, L. A. and C. T. Swift, "An Improved Model for the Dielectric Constant of Sea Water at Microwave Frequencies," Trans. IEEE AP-25 104-111 (1977).

9. Stogryn, A., "Equations for Calculating the Dielectric Constant of Saline Water," *Trans. IEEE, MTT-19* 733-736 (1971).
10. Jackson, J. D., "Classical Electrodynamics," John Wiley & Sons, Inc., New York (1962), p. 216ff.
11. Cardone, V. J., "Specification of the Wind Distribution in the Marine Boundary Layer for Wave Forecasting," Ph.D Thesis, New York University, Department of Meteorology and Oceanography, 1969 (Available from NTIS Order No. AD702490).
12. Cox, C. and W. Munk, "Some Problems in Optical Oceanography," *J. Marine Res.* 14, 63-78 (1955).
13. Nordberg, W., J. Conaway, D. B. Ross, and T. Wilheit, "Measurements of Microwave Emission from a Foam-Covered Wind Driven Sea," *J. Atmos. Sci.*, 38, 429-435 (1971).
14. Wilheit, T. T., "The Effect of Wind on the Microwave Emission From the Ocean's Surface at 37GHz," NASA TM-79588, July 1978, to be published in *J. Geophys. Res.*
15. Hollinger, J. P., "Passive Microwave Measurements of Sea Surface Roughness," *Trans. IEEE Geoscience Electronics, GE-9*, pp. 165-169 (1971).
16. Webster, W. J., Jr., T. T. Wilheit, D. B. Ross, and P. Gloersen, "Spectral Characteristics of the Microwave Emission from a Wind Driven Foam-Covered Sea," *J. Geophys. Res.* 81, 3095-3099 (1976).
17. Shutko, A., "Report on Soviet Progress in Microwave Radiometry of the Ocean's Surface," Presented at IUCRM Colloquium on Passive Radiometry of the Ocean's Surface, Patricia Bay, B.C., Canada, June 1978.
18. Blume, H-J. C., A. W. Love, M. J. Van Melle and W. W. Ho, "Radiometric Observations of Sea Temperature at 2.65GHz Over the Chesapeake Bay," *Trans-IEEE (AP)*, AP-25, 121-128, (1977).

19. Williams, G. F., "Microwave Emissivity Measurements of Bubbles and Foam," Trans-IEEE (GE), 9, 221-224, (1971).
20. Wilheit, T. T., "Radiative Transfer in a Plane Stratified Dielectric," Trans IEEE (GE), 16, 138-143, (1978).